

4.2.2.1

Airfoil Film Cooling



4.2.2.1-1 Introduction

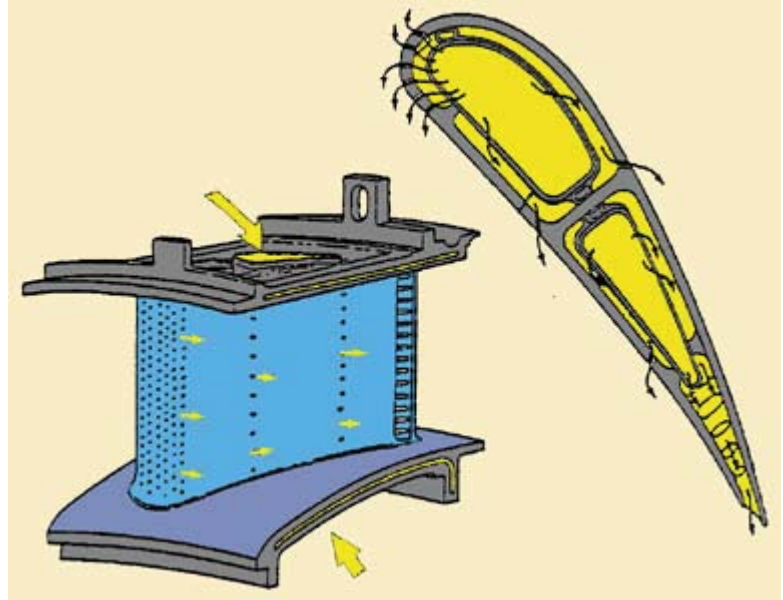


Fig. 1. Schematic of film cooling configurations on a vane

Source: (from <http://lttwww.epfl.ch/research/htprojects/filmcool.htm>)

Film cooling is a major component of the overall cooling of turbine airfoils. An example of a film cooled turbine vane is shown in figure 1¹. From the schematic of the airfoil in figure 1, it is evident that there are holes placed in the body of the airfoil to allow coolant to pass from the internal cavity to the external surface. The ejection of coolant gas through holes in the airfoil body results in a layer or “film” of coolant gas flowing along the external surface of the airfoil. Hence the term “film cooling” is used to describe the cooling technique. Since this coolant gas is at a lower temperature than the mainstream, the heat transfer into the airfoil is reduced. The adiabatic film effectiveness has a predominant effect in the design of the overall airfoil cooling. Consequentially, in this section details of film cooling performance are reviewed.

4.2.2.1-2 Fundamentals of Film Cooling Performance

The primary process by which film cooling reduces the heat transfer to the wall is by reducing the gas temperature near the wall, i.e. reducing the driving temperature potential for heat transfer to the wall. As the coolant flows from the coolant holes, it mixes with the mainstream gas resulting in an increase in coolant temperature. A typical example of this is presented in figure 2 which shows measurements of the temperature profile along the centerline of a coolant jet as it flows downstream of the coolant hole. In this figure the temperature contours are presented as normalized θ contours where θ is defined as:

$$\theta = \frac{T_{\infty} - T}{T_{\infty} - T_c} \quad (1)$$

where T is the local temperature, T_{∞} is the mainstream temperature, and T_c is the coolant temperature at the exit of the hole. Note that $\theta = 1$ is the normalized initial coolant temperature and $\theta = 0$ is the normalized mainstream temperature. The θ contours in figure 2 show that coolant quickly increases in temperature as it flows downstream. The coolant temperature at the wall will be at the adiabatic wall temperature, T_{aw} , and this temperature is generally assumed to be the driving temperature potential for heat transfer into the wall. Generally a normalized form of T_{aw} , referred to as the adiabatic effectiveness or film effectiveness, is used to characterize the film cooling performance. The film effectiveness, η , is defined as follows:

David G. Bogard

Mechanical Engineering Department
University of Texas at Austin
Austin, TX 78712

email: dbogard@mail.utexas.edu

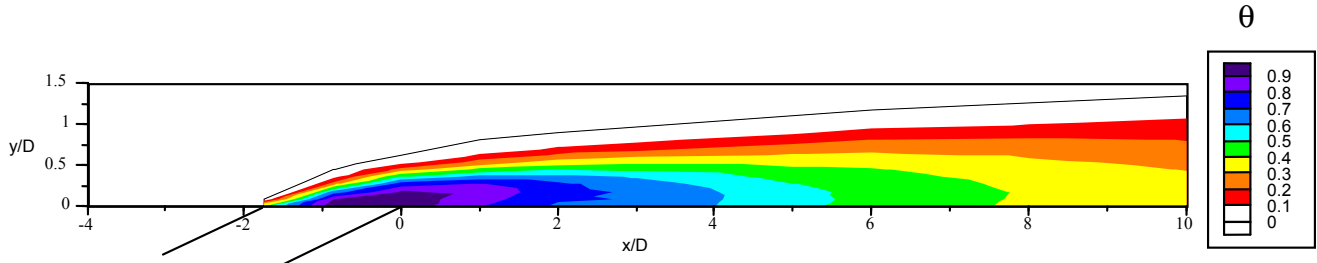


Fig. 2. Thermal profiles showing the coolant distribution flowing from a film cooling hole.

$$\eta = \frac{T_{\infty} - T_{aw}}{T_{\infty} - T_{c,exit}} \quad (2)$$

Where $T_{c,exit}$ is the coolant temperature at the coolant hole exit. For perfect film cooling performance, the film effectiveness would have a value of $\eta = 1.0$, i.e. T_{aw} would be equal to the coolant temperature at the exit of the hole; while a value of $\eta = 0$ would indicate that the film cooling has not reduced the gas temperature at the wall. In practice, η values decrease rapidly downstream of the coolant holes due to the strong turbulent dispersion of the coolant jet.

As mentioned above, typically T_{aw} is presumed to be the driving temperature potential for heat transfer into the wall. Consequently, the heat flux into the wall with film cooling, q_f'' , is determined using the heat transfer coefficient with film cooling, h_f , defined as follows:

$$h_f = q_f'' / (T_{aw} - T_w) \quad (3)$$

To evaluate the performance of the film cooling in reducing the heat flux to the wall, q_f'' should be compared to the local heat flux to the wall that would occur without film cooling, i.e. q_0'' that is determined based on the heat transfer coefficient without film cooling, h_0 , using the following:

$$q_0'' = h_0(T_{\infty} - T_w) \quad (4)$$

Examining equations (3) and (4), it is apparent that a reduced temperature for T_{aw} relative to T_{∞} will result in a reduced heat flux to the wall. However, these equations also highlight that there is potentially a difference in heat transfer coefficients for the film cooling case and the no-film cooling case. In fact, the disturbance caused by the injection of coolant often causes an increase in the heat transfer coefficient. This increase in heat transfer coefficient causes an increase in heat transfer to the wall, and hence is detrimental. Consequently the overall performance of the film cooling configuration needs to be evaluated in terms of the a net heat flux reduction which takes into account decreased gas temperature provided by the coolant film and the increased heat transfer coefficient due to the coolant injection process.

This net heat flux reduction, Δq_r , is obtained by combining equations (3) and (4) resulting in the following:

$$\Delta q_r = 1 - \frac{q_f''}{q_0''} = 1 - \frac{h_f(T_{aw} - T_w)}{h_0(T_{\infty} - T_w)} \quad (5)$$

which can be rewritten as:

$$\Delta q_r = 1 - \frac{h_f}{h_0} \left(1 - \frac{\eta}{\phi} \right) \quad (6)$$

where ϕ is the non-dimensional metal temperature for the operational turbine airfoil, and is defined as follows:

$$\phi = \frac{T_{\infty} - T_w}{T_{\infty} - T_{c,internal}} \quad (7)$$

where $T_{c,internal}$ is the coolant temperature inside the internal cooling passages of the turbine airfoil. Note that ϕ is an unknown that is not generally determined in the laboratory experiment, and a value for ϕ must be assumed in order to estimate a net heat flux reduction using equation (6). A typical value for operational film cooled turbine airfoils is $\phi = 0.6$, and this value is generally assumed when analyzing laboratory data.

4.2.2.1-3 Correlations of Film Cooling Performance

The primary measure of film cooling performance is the film effectiveness, η , since this has a dominating effect on the net heat flux reduction. Furthermore, industrial designers typically will focus on the laterally averaged film effectiveness, $\bar{\eta}$, which is the average η over a line normal to the flow and extending a distance equal to the pitch between holes. Besides the simplification in processing film effectiveness results by using only laterally averaged data, there is a physical rationale for using only the laterally averaged film effectiveness. Recall that η represents the normalized adiabatic wall temperature which corresponds to the gas temperature adjacent to the surface. As the coolant jet flows downstream of the coolant hole there is a large spatial variation of gas temperature near the wall as is evident by the contour plots η shown in figure 3. However the large conductivity of the metal turbine airfoil causes a much more uniform distribution of the “metal temperature”. Consequently the laterally averaged film effectiveness is a reasonable representation of the effect of the coolant jet², and most of the correlations for film effectiveness presented in this section are in terms of laterally averaged cooling effectiveness. However, it should be recognized that for purposes of understanding the physical processes of coolant dispersion, and for validation and improvement of computational predictions, the spatial distribution of η is important information.

Ideally a film of coolant would be introduced to the surface of an airfoil using a slot angled almost tangential to the surface in order to provide a uniform layer of coolant that remain attached to the surface. However, long slots in the airfoil would seriously reduce the structural strength of the airfoil, and hence are not feasible. Consequently coolant is typically introduced to the airfoil surface using rows of holes. The film cooling performance is dependent on the hole geometry and configuration of the layout of the holes. Furthermore, various factors associated with the coolant and mainstream flows, and the airfoil geometry, also significantly affect the cooling performance. A listing of the various factors influencing film cooling performance is presented in table 1³. Considering the many factors listed in table 1, the difficulty in predicting film cooling performance is evident. The effects of these factors are discussed in the following subsections.

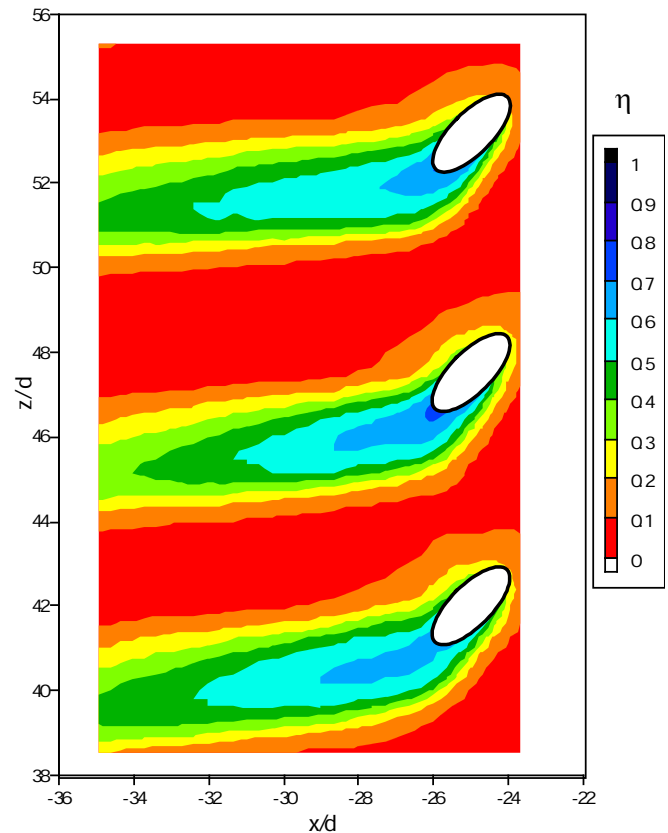


Fig. 3. Typical film effectiveness contours.

Film Effectiveness at Varying Blowing Ratios

In the following description of film cooling performance, a baseline geometry of cylindrical holes spaced $3d$ apart and inclined 30° to the surface and aligned in the flow direction is used. A comprehensive study of the film effectiveness for this configuration was done by Baldauf et al. using a flat, smooth surface test facility⁴. Results for a range of blowing ratios are presented in figure 4. The blowing ratio, M , is the ratio of the coolant mass flux to the mainstream mass flux and is defined as follows:

$$M = \frac{\rho_c U_c}{\rho_\infty U_\infty} \quad (8)$$

where ρ_c and ρ_∞ are the coolant and mainstream density, respectively, and U_c and U_∞ are the coolant and mainstream velocity, respectively. Figure 4 shows that the level of $\bar{\eta}$ increases systematically with an increase in M until $M = 0.6$, but for $M \geq 0.85$, the peak level of $\bar{\eta}$ begins to decrease, and the position of the peak moves downstream. The initial increase in $\bar{\eta}$ with increasing M is expected due to the greater mass flow of coolant. The decrease in $\bar{\eta}$ for $M \geq 0.85$ is due to the coolant jet separating from the surface. This is graphically illustrated in the sequence of thermal profile measurements presented in figure 5 (generated from data from Thole, Sinha, Bogard & Crawford⁵) showing the non-dimensional temperature along the centerline of a coolant jet exiting a cylindrical coolant hole inclined 35° to the surface. Three blowing rates are presented, but they are identified in terms of the momentum flux ratio I which is defined as follows:

4.2.2.1 Airfoil Film Cooling

Table 1 Factors Affecting Film Cooling Performance

Coolant/Mainstream Conditions	Hole Geometry and Configuration	Airfoil Geometry
Mass flux ratio*	Shape of the hole*	Hole location - leading edge - main body
Momentum flux ratio*	Injection angle and compound angle of the coolant hole *	- blade tip - endwall
Mainstream turbulence*	Spacing between holes, P/d	Surface curvature*
Coolant density ratio	Length of the hole, l/d	Surface roughness*
Approach boundary layer	Spacing between rows of holes and number of rows	
Mainstream Mach number		
Unsteady mainstream flow		
Rotation		

* Factors that have a significant effect on predictability of film cooling performance.

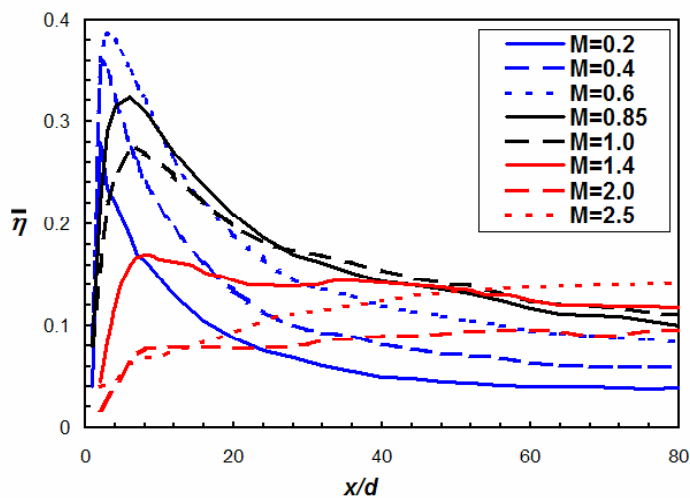


Fig. 4. Distributions of $\bar{\eta}$ for varying blowing ratios presented as a function of the streamwise distance x/d (reproduced with permission from *Journal of Turbomachinery*).

Source: reproduced from Figure 2(b) in Baldauf et al. (see note 4).

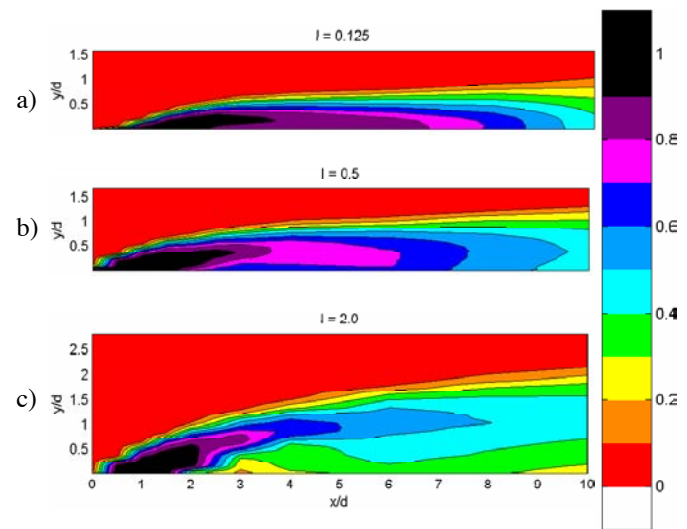


Fig. 5. Thermal profiles showing three states of coolant jets: attached, detached then reattached, and fully detached (reproduced with permission from Hemisphere Publishing Corporation).

Source: See note 5.

The three profiles presented in figure 5 represent samples of three states for the coolant jets⁶: (a) fully attached coolant jets shown in fig. 5a, (b) coolant jets that detached then reattached shown in fig. 5b, and (c) coolant jets that were fully detached shown in fig. 5c. Clearly as the coolant jets begin to detach the coolant temperature at the wall decreases (θ increases) as the core of the coolant jet travels above the surface. The range of momentum flux ratios for each of these flow states was found to be $I < 0.4$ for fully attached jets, $0.4 < I < 0.8$ for detached/reattached jets, and $I > 0.8$ for fully detached jets for flat surface flows⁷. Clearly, whether or not the coolant jets are attached strongly affects the cooling performance.

To first order, the film effectiveness performance for varying blowing ratios can be scaled using the parameter x/MS_e where S_e is the “equivalent slot length” with $S_e = A_{hole}/P$ where A_{hole} is the cross-sectional area of the coolant hole and P is the pitch between holes⁸. The $\bar{\eta}$ distributions for the Baldauf et al. data shown in figure 4 presented in terms of the x/MS_e parameter are shown in figure 6⁹. At first this does not appear to collapse the data; but, if results are considered only for $0.2 < M < 0.85$, then there is a good collapse of the $\bar{\eta}$ profiles. These measurements were made using coolant with a density ratio of $DR = 1.8$, and consequently the blowing ratio of $M = 0.85$ corresponds to a momentum flux ratio of $I = 0.4$. As will be shown below, coolant jets with $I > 0.4$ are in blowing regimes where there is detachment of the coolant jets. Consequently, the $\bar{\eta}$ performance scales well with x/MS_e when the coolant jets are attached, i.e. $I \leq 0.4$. For prediction of film effectiveness for higher blowing ratios, Baldauf et al. developed more sophisticated correlation techniques that will not be detailed here¹⁰.

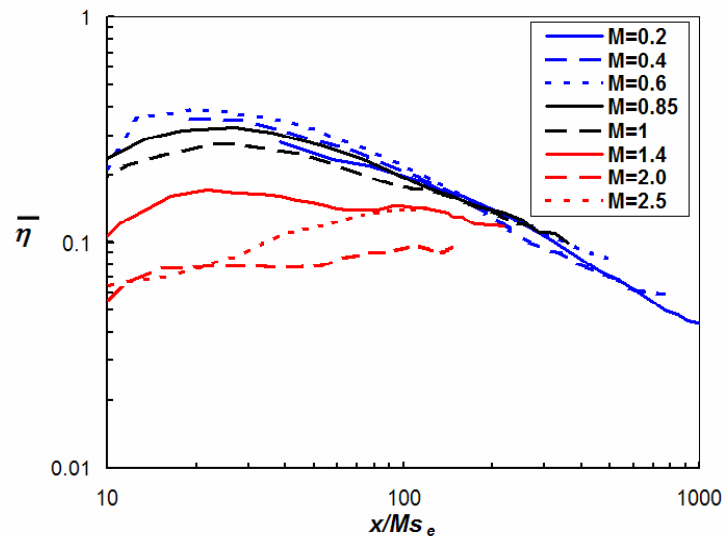


Fig. 6. Distributions of $\bar{\eta}$ for varying blowing ratios presented as a function of the x/MS_e parameter (reproduced with permission from *Journal of Turbomachinery*).

Source: reproduced from Figure 7 (a) in Baldauf et al. (See note 4.)

Film Effectiveness at Density Ratios

Typically the coolant to mainstream density ratio for engine conditions is $DR \approx 2$, but often experimental measurements of film cooling performance are conducted with density ratios that are much smaller, even with $DR \approx 1$. Because of this range of density ratios used in testing, it is valuable to understand how the coolant density ratio affects film cooling performance. When testing with lower density ratios, coolant flows at a given mass flux ratio will have higher velocity and momentum flux ratios. Recall that coolant jet separation is primarily a function of momentum flux ratio, so lower density coolant jets will tend to separate before higher density ratio jets. Consequently the maximum film effectiveness for lower density ratio coolant jets is less than for the higher density ratio jets, but the difference in film effectiveness levels is generally small. For example, Sinha et al., Pederson et al., and Baldauf et al. found that the maximum laterally averaged film effectiveness was nominally 20% higher for coolant $DR \approx 2$ compared to $DR \approx 1.2$ near the hole ($x/d < 20$) but was essentially the same farther downstream¹¹. These tests were for smooth, flat surfaces. Tests for a vane leading edge, pressure side and highly curved suction side showed similar film effectiveness for low and high density coolant, but the low density ratio coolant has 10% lower film effectiveness in some cases¹².

For low momentum flux ratios where coolant jets are fully attached, film effectiveness performance for low density coolant is essentially the same as for high density coolant when compared at the same mass flux (blowing) ratio. However, at higher momentum ratios where the coolant jets begin to detach, $I > 0.4$, the film effectiveness for low and high density ratio coolant jets are most similar for similar I . However, for showerhead blowing, film effectiveness for low and high density ratio coolant is best matched using M for all blowing ratios¹³.

4.2.2.1 Airfoil Film Cooling

Heat Transfer Coefficients

The disturbance to the flow caused by coolant injection might be expected to increase heat transfer coefficients downstream of the coolant holes. Generally this is true, but the increase in heat transfer coefficient relative to the no-blowing case is relatively small, less than 5% beyond $x/d = 5$, for momentum flux ratios of $I < 0.3$ ¹⁴. For higher momentum flux ratios the heat transfer coefficient can be increased by 10% to 20%, but these higher momentum flux ratios are not likely to be used because of poor film effectiveness. Most studies of heat transfer coefficients were done with low density ratio coolant, but results showed that the effects on the heat transfer coefficient were not very sensitive to the density ratio, with the lower density ratio coolant causing a larger increase due to the higher momentum for lower density ratio coolant¹⁵.

4.2.2.1-4 Effects of Hole Geometry and Configuration on Film Cooling Performance

As described in table 1, there are many hole geometry and configuration variables that affect film cooling performance. Compound angle injection and shaped holes have major effects on film cooling performance and will be discussed in this section. This is a summary of a more comprehensive review of the effects of the varying hole configurations presented in "Gas Turbine Film Cooling"¹⁶.

Film Cooling with Compound Angle Holes

For the baseline case described above, the coolant holes were angled such that the exiting coolant jets are parallel with the mainstream direction. When the coolant hole is angled to the mainstream direction, this is referred to as "compound angle" injection. Compound angles can be as much as 90° , i.e. normal to the mainstream direction. Coolant injected at a compound angle is quickly turned to the mainstream direction, but will generally have a broader distribution of coolant. Furthermore, the coolant presents a broader profile to the mainstream so that the mainstream has a larger impact on the jet more effectively turning the jet towards the wall. This inhibits jet separation, and results in better film effectiveness for the compound angle holes at higher blowing ratios. Film effectiveness performance for 90° compound angle holes compared to of 0° (streamwise oriented holes), shown in figure 7, illustrates this point. These data are for cylindrical holes spaced $6.5d$ apart on a smooth flat test surface with low mainstream turbulence levels. Maximum film effectiveness for the 90° compound angle holes was similar to that for the 0° holes and occurred at a similar momentum flux ratio. However the 90° compound angle holes sustained high film effectiveness for very high blowing ratios. For momentum flux ratios greater than $I = 1.0$, the film effectiveness for the 90° compound angle holes was a factor of 2 to 3 higher than that for the streamwise-oriented holes. Although the film effectiveness for compound angle holes is significantly better than for streamwise-oriented holes at high momentum flux ratios, the net heat flux reduction for compound angle holes is similar to the streamwise-oriented holes¹⁷. This is illustrated in figure 8 for 90° compound angle holes. At the higher momentum flux ratio of $I = 1.1$ the average $\Delta\bar{q}_r$ over the $90d$ distance downstream of the coolant holes was about the same for 90° and 0° compound angle holes. The similarity of the net heat flux reduction even though the film effectiveness is much greater for 90° compound angle holes is due to a greater increase in heat transfer coefficient for these holes compared to streamwise-oriented holes. Even though the average increase in heat transfer coefficient by the compound angle holes was only 10%, this was sufficient to offset the improved film effectiveness.

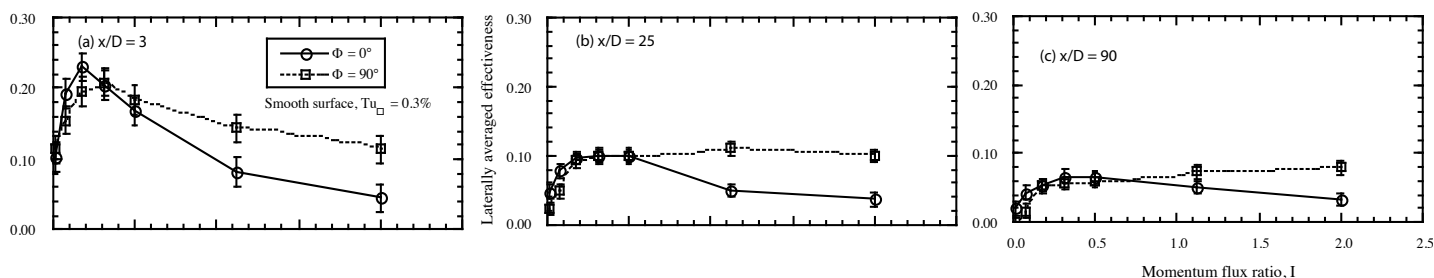


Fig. 7. Comparison of streamwise and laterally directed holes in terms of laterally averaged effectiveness as a function of momentum flux ratio for a smooth surface and low free-stream turbulence

Source: See note 14 (Schmidt & Bogard).

Film Cooling with Shaped Holes

Improved film effectiveness can be achieved if the exit of the hole is expanded so that coolant is slowed through a diffuser. Examples of shapes investigated in the open literature are shown in figure 9. There are two advantages for such a "shaped hole": the coolant exit velocity is reduced and a broader jet cross-section is presented to the mainstream flow. Both these characteristics will reduce the tendency for the coolant jet to separate. This results in good film effectiveness levels for shaped holes at very high blowing ratios as shown in figure 10. These data were obtained with a row of coolant holes angled 30° with the surface and spaced $4d$ apart. The spatially averaged film effectiveness, η , was based on an average from $x/d = 2$ to 22. The blowing ratio for this figure is based on the average

velocity of the coolant at the inlet to the coolant hole, so the mass flow of coolant for the cylindrical and shaped holes are the same for the same M . Film effectiveness for cylindrical holes begins to decrease for $M > 0.7$ which corresponds to a momentum flux ratio of $I > 0.3$ given that the density ratio for these tests was $DR = 1.7$. This decrease is due to separation of the coolant jets. In contrast the film effectiveness for the shaped holes continues to increase for blowing ratios up to $M = 2.5$ ($I = 3.7$) showing that the diffusing hole shape is very effective in keeping the coolant jets attached.

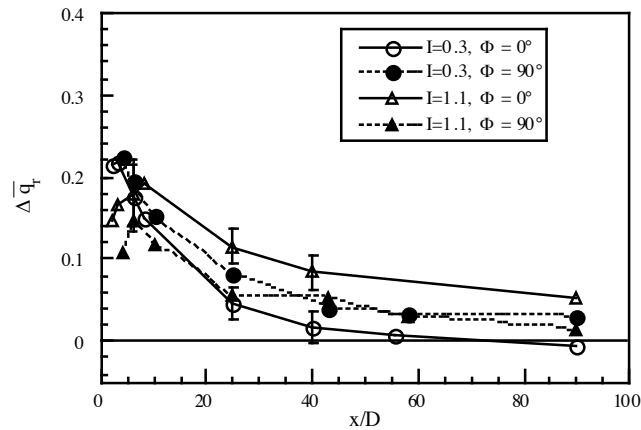


Fig. 8. Comparison of streamwise and laterally directed holes in terms of net heat flux reduction for a smooth surface and high free-stream turbulence.

Source: See note 14 (Schmidt & Bogard).

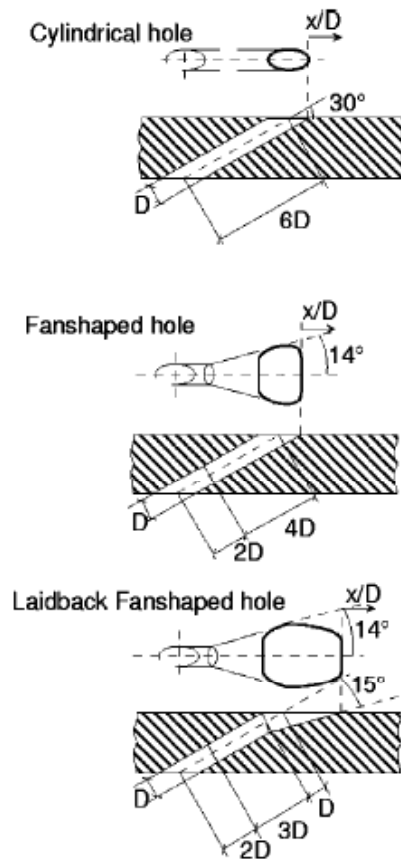


Fig. 9. Schematics of different cooling hole shapes (reproduced with permission from *Journal of Turbomachinery*).

Source: C. Saumweber, A. Schulz, and S. Wittig, "Free-Stream Turbulence Effects on Film Cooling with Shaped Holes," *Journal of Turbomachinery* 125 (2003): 65-73.

4.2.2.1 Airfoil Film Cooling

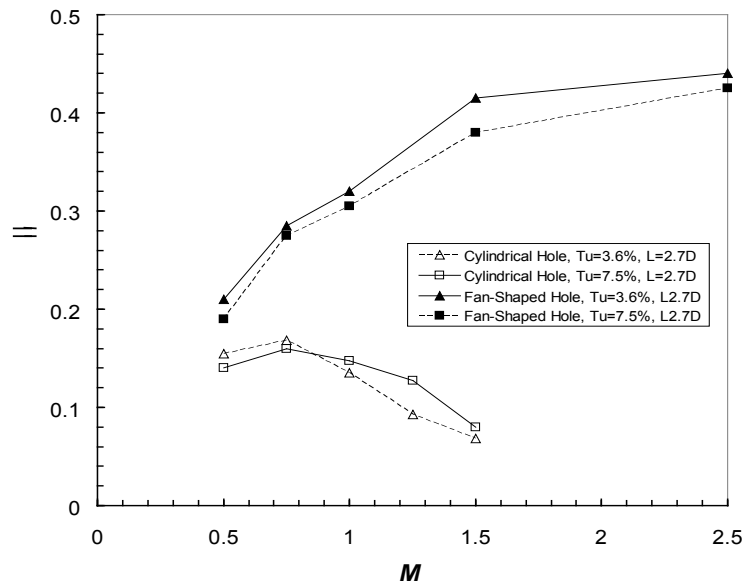


Fig. 10. Comparison of spatially averaged cooling effectiveness for cylindrical holes and shaped holes (reproduced with permission from *Journal of Turbomachinery*).

Source: same as for fig. 9.

4.2.2.1-5 Airfoil Surface Effects on Film Cooling Performance

Surface curvature and surface roughness are significant factors affecting film cooling performance. Clearly for turbine airfoils strong convex curvature exists around the leading edge and along the suction side of the airfoil. Sometimes strong concave curvature is encountered on the pressure side of the airfoils. Surface roughness varies with the length of operation of the engine; new airfoils are relatively smooth, but after some period of operation the surfaces can become quite rough due to erosion, spallation of thermal barrier coatings, and deposition of contaminants. The following is a brief review of these surface effects.

Surface curvature

Several studies have shown that surface curvature can significantly change film effectiveness; convex curvature increasing η and concave curvature decreasing η at typical operational blowing ratios¹⁸. The effects of varying strengths of curvature are demonstrated in figure 11 in which the laterally averaged film effectiveness, $\bar{\eta}$, at $x/d = 40$ are presented for a range of curvatures, $46 < 2r/d < 126$, with zero pressure gradient (r is the radius of curvature for the surface). These studies indicated that an increased convex curvature (decreasing $2r/d$) greatly enhances film effectiveness, while concave curvature decreases film effectiveness except at high momentum flux ratios. These effects of surface curvature can be explained by the wall normal pressure gradients that necessarily exist with wall curvature. When the momentum of the jet tangential to the wall is less than the mainstream momentum the normal pressure gradients drive the coolant jets towards or away from the wall for convex and concave curvature, respectively. For convex curvature, the inward pressure broadens the coolant distribution by pressing the jet to the wall, and keeps the jet attached for higher momentum flux ratios. For concave curvature the opposite occurs, i.e. the coolant jets are pushed away from the wall.

Surface Roughness

Significant increases in surface roughness during typical operating conditions have been reported by several studies¹⁹, with maximum roughness levels as high as $Re_k = 500$ where Re_k is the equivalent sandgrain roughness Reynolds number²⁰. Given that “fully rough” conditions exist when $Re_k > 70$, this roughness level is extremely large. Also, maximum roughness heights were observed to be greater than $250 \mu\text{m}$, which is $0.5d$ for typical coolant hole diameters. Surface roughness degrades film cooling performance by increasing the heat transfer coefficient and potentially reducing film effectiveness. Heat transfer coefficients can be increased by as much as 50% to 100%²¹. Studies of the effects of surface roughness on film effectiveness using flat surface facilities²² showed small reductions (<10%) of average film effectiveness for lower blowing ratios, and small increases for high blowing ratios. However, a study of roughness effects on film effectiveness on the suction side of a vane²³ showed surface roughness decreased film effectiveness by as much as 25% at the optimum blowing ratio, but increased film effectiveness as much as 50% at higher blowing ratios. The decrease in film effectiveness at the optimum blowing ratio was primarily due to the roughness upstream of the coolant holes. The upstream roughness doubled the boundary layer thickness and significantly increased turbulence levels which resulted in more separation of the coolant jets and increased dispersion of the coolant.

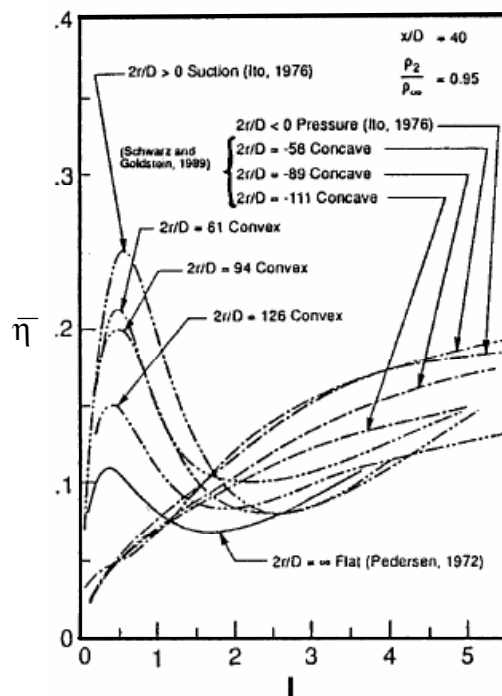


Fig. 11. Effect of convex and concave curvature on film effectiveness (reproduced with permission from *Journal of Turbomachinery*).

Source: see note 18 (Schwarz, Goldstein, and Eckert).

4.2.2.1-6 Mainstream Effects on Film Cooling Performance

There are a number of mainstream factors that can affect film cooling performance including approach boundary layers, turbulence levels, Mach number, unsteadiness, and rotation²⁴. Because of the very high levels of mainstream turbulence exiting the combustor and entering the turbine section, turbulence levels have the largest effect on film cooling performance. Mainstream turbulence levels exiting the combustor can be higher than $Tu = 20\%$ and have been found to be nominally isotropic in simulated combustor studies²⁵. Furthermore the integral length scale of the turbulence is large relative to the coolant hole diameters, i.e. $\Lambda_f/d > 10$ (based on Λ_f values given in Radomsky and Thole²⁶). Primarily due to the acceleration of the mainstream as it passes around the first vane, the local turbulence levels reduce to less than 5% on the suction side of the vane, and to about 10% for much of the pressure side. These are still relatively high turbulence levels, and it is important to recognize the effects on film cooling performance.

High mainstream turbulence levels degrade film cooling performance by increasing heat transfer coefficients and generally decreasing film effectiveness. Simulations of the large scale turbulence with levels of $Tu = 10\%$ to 17% showed an increase in heat transfer coefficient of 15% to 30%, respectively²⁷. The effects of high mainstream turbulence levels on film effectiveness are shown by the laterally averaged film effectiveness levels for $Tu = 0.3\%$, 10% , and 20% shown in figure 12. Results in figure 12 were obtained using a flat surface test facility with a row of cylindrical holes spaced $6.5d$ apart, with an injection angle of 30° and aligned with the mainstream direction. Smooth and rough surfaces were tested. The coolant density ratio was $DR = 2.0$. For a smooth surface with low turbulence levels the optimum momentum flux ratio was $I = 0.3$. At this momentum flux ratio, a turbulence level of $Tu = 17\%$ caused a factor of two decrease in film effectiveness near the hole, and almost a complete loss of cooling for $x/d > 25$. The optimum momentum flux ratio for high mainstream turbulence conditions was about $I = 1.1$, substantially higher than would have been expected from low mainstream turbulence tests. At this higher momentum flux ratio the film effectiveness for the high mainstream turbulence case was higher than for the low mainstream turbulence case. This difference was attributed to the higher mainstream turbulence mitigating the effect of coolant jet separation by returning some of the coolant towards the surface with the increased coolant dispersion caused by the higher turbulence levels. These results show the importance of accounting for realistic mainstream turbulence levels when predicting film cooling performance.

4.2.2.1-7 Airfoil Leading Edge Film Cooling

Film cooling of the leading edge of vanes and blades is distinctly different than film cooling of the aft-body of the airfoils because coolant is injected into a stagnation region rather than into a cross-flow. Furthermore, the heat loads are typically much larger along the leading edge, so generally a dense array of coolant holes is used around the leading edge. This array of holes around the leading edge is referred to as the “showerhead” and generally consists of six to eight rows of holes for vanes and three to five rows of holes for blades. Holes are typically aligned radially, i.e. normal to the mainstream direction, with injection angles relative to the surface ranging from 20° to 45°.

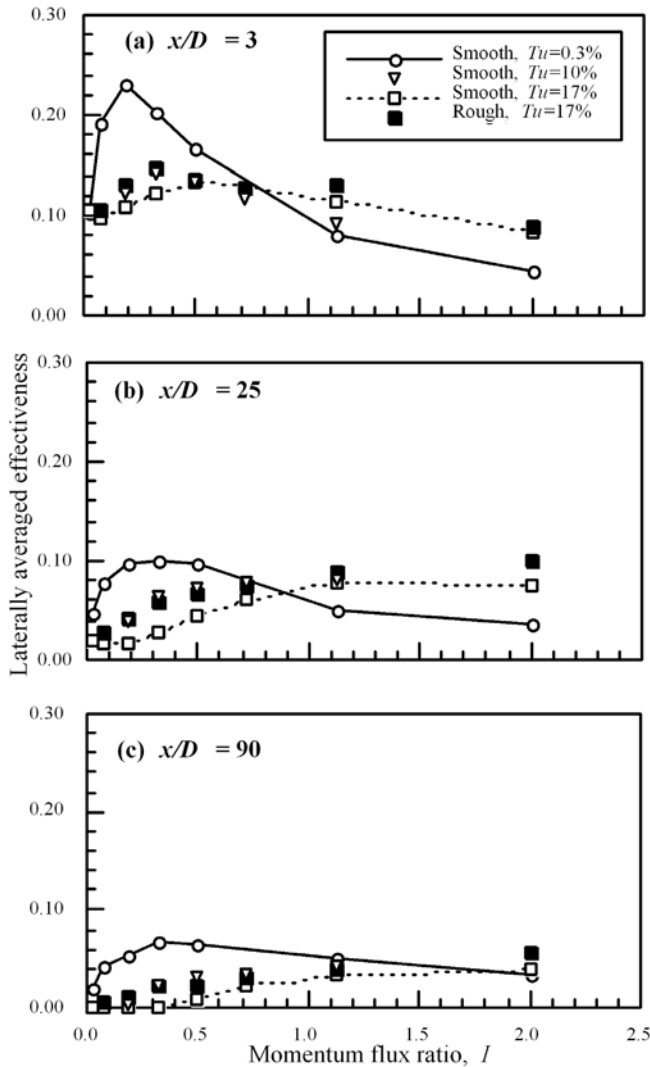


Fig. 12. Effect of freestream turbulence level on laterally averaged effectiveness as a function of momentum flux ratio for a smooth surface and low free-stream turbulence

Source: D.L. Schmidt and D.G. Bogard, “Effects of Free-Stream Turbulence and Surface Roughness on Film Cooling,” ASME Paper 96-GT-462, 1996.

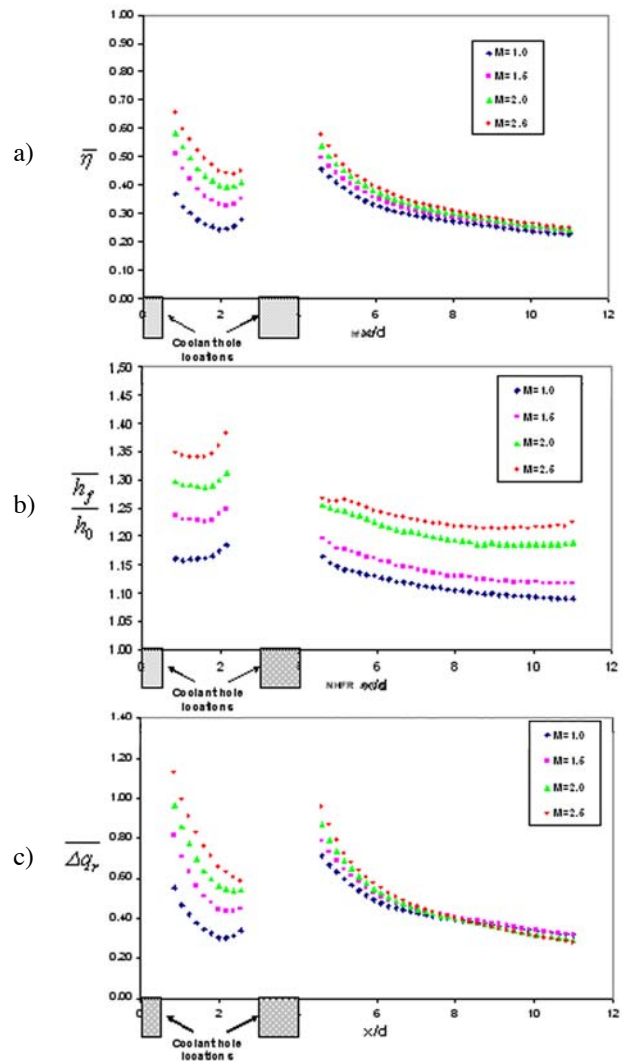


Fig. 13. Film cooling performance for a simulated blade leading edge with three rows of holes. Mainstream turbulence was $Tu = 10\%$. Stagnation line coolant holes at $x/d = 0$. Performance in terms of (a) laterally averaged heat effectiveness, (b) laterally averaged heat transfer coefficient augmentation, and (c) laterally averaged net heat transfer reduction.

Source: See note 2.

Film cooling performance for a simulated blade leading edge is presented in figure 13 in terms of the laterally averaged film effectiveness, $\bar{\eta}$, heat transfer coefficient increase, h/h_o , and net heat flux reduction, $\Delta\bar{q}_r$ ²⁸. These data were measured using a simulated blade leading edge with a three-row coolant hole configuration with “laid back” shaped holes oriented radially, an injection angle of 20°, and a spacing between holes of 7.6*d*. Blowing ratios were based on the approach velocity to the leading edge and ranged from $M = 1.0$ to 2.5. As shown in figure 13, film effectiveness continues to increase with increasing blowing ratio. Coolant injection caused a 10% to 35% increase in heat transfer coefficients. Finally the net heat flux reduction mirrored the film effectiveness performance. High levels of net heat flux reduction can be attributed to the high levels of film effectiveness.

4.2.2.1-8 Notes

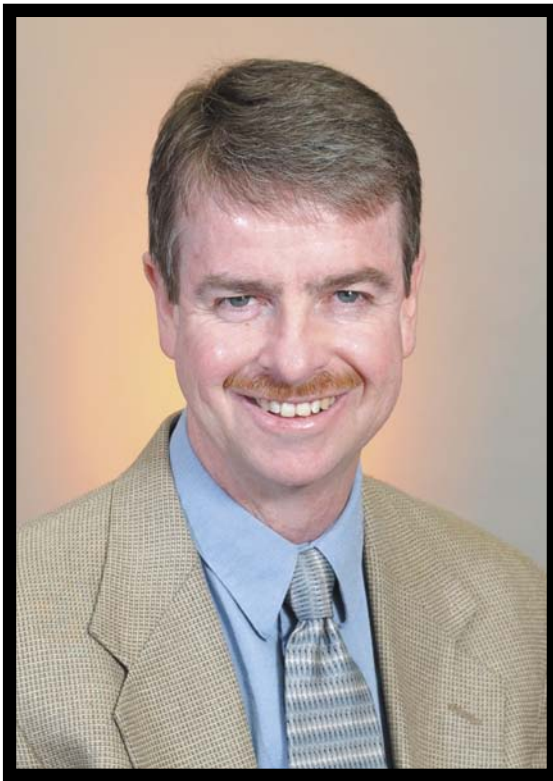
1. Figure from web site: <http://littwww.epfl.ch/research/htprojects/filmcool.htm>
2. B.D. Mouzon, E.J. Terrell, J.E. Albert, and D.G. Bogard, “Net Heat Flux Reduction and Overall Effectiveness for a Turbine Blade Leading Edge,” ASME paper GT2005-69002, 2005.
3. D. G. Bogard and K.A. Thole, “Gas Turbine Film Cooling,” accepted AIAA Journal of Propulsion and Power, 2006.
4. S. Baldauf, M. Scheurlen, A. Schulz, and S. Wittig, “Correlation of Film-Cooling Effectiveness from Thermographic Measurements at Enginelike Conditions,” *Journal of Turbomachinery* 124 (2002): 686-698.
5. K.A. Thole, A. Sinha, D. G. Bogard, and M. E. Crawford, “Mean Temperature Measurements of Jets with a Crossflow for Gas Turbine Film Cooling Application,” *Rotating Machinery Transport Phenomena*, J. H. Kim and W. J. Yang, ed. Hemisphere Publishing Corporation, New York, New York, 1992.
6. Ibid.
7. Ibid.
8. R. J. Goldstein, “Film Cooling,” *Advances in Heat Transfer* 7 (1971): 321-380.
9. See note 4 above.
10. Ibid.
11. A.K. Sinha, D.G. Bogard, and M.E. Crawford, “Film Cooling Effectiveness Downstream of a Single Row of Holes with Variable Density Ratio,” *ASME Journal of Turbomachinery* 113, no. 3 (1991): 442-449; D.R. Pedersen, E. Eckert, and R. Goldstein, “Film Cooling with Large Density Differences Between the Mainstream and the Secondary Fluid Measured by the Heat-Mass Transfer Analogy,” *ASME Journal of Heat Transfer* 99 (1977): 620-627; also see note 4 above.
12. Cutbirth, J. and Bogard, D., “Effects of Coolant Density Ratio on Film Cooling,” ASME Gas Turbine Expo, GT2003-38582, Atlanta, Georgia, June, 2003, pp 1-10; M. I. Ethridge, J.M. Cutbirth, and D.G. Bogard, “Scaling of Performance for Varying Density Ratio Coolants on an Airfoil with Strong Curvature and Pressure Gradients,” *ASME Journal of Turbomachinery* 123, (2001): 231-237.
13. See note 12 above (Cutbirth).
14. V.L. Eriksen and R. Goldstein, “Heat Transfer and Film Cooling Following Injection Through Inclined Circular Tubes,” *ASME Journal of Heat Transfer* 96, no.1 (1974): 239-245; Schmidt, D.L. and Bogard, D.G., “Effects of Free-Stream Turbulence and Surface Roughness on Laterally Injected Film Cooling,” *Proceedings of the 32nd National Heat Transfer Conference, HTD-Vol. 350, vol. 12, pp. 233-244, 1997.*
15. S. Baldauf, M. Scheurlen, A. Schulz, and S. Wittig, “Heat Flux Reduction From Film Cooling and Correlation of Heat Transfer Coefficients from Thermographic Measurements at Enginelike Conditions,” *Journal of Turbomachinery* 124 (2002): 699-709
16. See note 3 above.
17. B. Sen, D.L. Schmidt, and D.G. Bogard, “Film Cooling with Compound Angle Holes: Heat Transfer,” *ASME Journal of Turbomachinery* 118, no. 4 (1996): 800-806; also see note 14 (Schmidt).
18. S. Ito, R. Goldstein, and E. Eckert, “Film Cooling of a Gas Turbine Blade,” *Journal of Engineering for Power* 100 (1978): 476-481; S. Schwarz, R. Goldstein, and E. Eckert, “The Influence of Curvature on Film Cooling Performance,” *Journal of Turbomachinery* 112 (1990): 472-478.
19. J.P. Bons, R. Taylor, S. McClain, and R.B. Rivir, “The Many Faces of Turbine Surface Roughness,” *Journal of Turbomachinery* 123 (2001): 739-748; D.G. Bogard, D.L. Schmidt, and M. Tabbita, “Characterization and Laboratory Simulation of Turbine Airfoil Surface Roughness and Associated Heat Transfer,” *Journal of Turbomachinery* 120 (1998): 337-342.
20. D.G. Bogard, D. Snook, and A. Kohli, “Rough Surface Effects on Film Cooling of the Suction Side Surface of a Turbine Vane,” ASME Paper No. EMECE2003-42061, 2003.

4.2.2.1 Airfoil Film Cooling

21. J.L. Rutledge, D. Robertson, and D.G. Bogard, "Degradation of Film Cooling Performance on a Turbine Vane Suction Side Due to Surface Roughness," ASME Gas Turbine Expo, GT2005-69045, 2005; also see note 19 (Bogard).
22. R.J. Goldstein, E.R.G. Eckert, H.D. Chiang, and E. Elovic, "Effect of Surface Roughness on Film Cooling Performance," *Journal of Engineering for Gas Turbines and Power* 107 (1985): 111-116; D.L. Schmidt, B. Sen, and D.G. Bogard, "Effects of Surface Roughness on Film Cooling," ASME Paper No. 96-GT-299, 1996.
23. See note 20 and 21.
24. See note 3.
25. R.W. Radomsky and K.A. Thole, "Flowfield Measurements for a Highly Turbulent Flow in a Stator Vane Passage," *Journal of Turbomachinery* 122 (2000): 255-262.
26. Ibid.
27. See note 19 (Bogard).
28. J. E. Albert, F. Cunha, and D. G. Bogard, "Adiabatic and Overall Effectiveness for a Film Cooled Blade," ASME Paper GT2004-53998, 2004.

BIOGRAPHY

4.2.2.1 Airfoil Film Cooling



David G. Bogard

Mechanical Engineering Department
University of Texas at Austin
Austin, TX 78712

email: dbogard@mail.utexas.edu

Dr. David Bogard is a Professor of Mechanical Engineering at the University of Texas at Austin, and holds the John E. Kasch Fellow in Engineering. He received his B.S. and M.S. degrees in Mechanical Engineering from Oklahoma State University, and his Ph.D. from Purdue University. He has served on the faculty at the University of Texas since 1982. Dr. Bogard has been active in gas turbine cooling research since 1986, and has published over 100 peer-reviewed papers. He was awarded the ASME Heat Transfer Committee Best Paper Award in 1990 and 2003, and is a fellow of the ASME.